REPORT DOCUMENTATION PAGE

Form Approved
OMB No. 0704-0188

1. REPORT DATE *(DD-MM-YYYY)*	**2. REPORT TYPE**	**3. DATES COVERED** *(From - To)*
01-08-2018	Journal Article	10-01-2017 – 08-01-2018

4. TITLE AND SUBTITLE
Eye Safety Implications of High Harmonic Generation in Zinc Selenide

5a. CONTRACT NUMBER
FA8650-14-D-6519

5b. GRANT NUMBER

5c. PROGRAM ELEMENT NUMBER

6. AUTHOR(S)
C.B Marble, S.P. O'Connor, D.T. Nodruft, V.V. Yakovlev, and A.W. Wharmby

5d. PROJECT NUMBER

5e. TASK NUMBER

5f. WORK UNIT NUMBER
H0RY

7. PERFORMING ORGANIZATION NAME(S) AND ADDRESS(ES)

Air Force Research Laboratory
711th Human Performance Wing
Airman Systems Directorate
Bioeffects Division
Optical Radiation Bioeffects Branch

Engility Corporation
4141 Petroleum Rd
JBSA Fort Sam Houston TX

8. PERFORMING ORGANIZATION REPORT NUMBER

9. SPONSORING / MONITORING AGENCY NAME(S) AND ADDRESS(ES)
Air Force Research Laboratory
711th Human Performance Wing
Airman Systems Directorate
Bioeffects Division
Optical Radiation Bioeffects Branch
4141 Petroleum Rd
JBSA Fort Sam Houston TX

10. SPONSOR/MONITOR'S ACRONYM(S)

11. SPONSOR/MONITOR'S REPORT NUMBER(S)
AFRL-RH-FS-JA-2019-0001

12. DISTRIBUTION / AVAILABILITY STATEMENT
Distribution A: Approved for public release (PA); distribution unlimited. PA Case No: TSRL-PA-2018-0212 Date Cleared: 10-03-2018

13. SUPPLEMENTARY NOTES

14. Abstract

Polycrystalline zinc selenide (ZnSe) has been the subject of many nonlinear optics studies for wavelengths under 4.0 μm including sum/difference frequency generation, harmonic generation, and filamentation. This letter documents a systematic study of the conversion efficiency of high harmonic generation (HHG) in ZnSe for mid-infrared wavelengths ranging from 2.7 μm to 8.0 μm. By using longer excitation wavelengths and higher intensities than previous studies, HHG through the twelfth harmonic is observed. The high conversion efficiency of mid-infrared to near-infrared light in ZnSe raises concerns of a nonlinear retinal hazard. We contrast the HHG behavior of ZnSe against the observed harmonic generation of calcium fluoride, BK7, and fused silica over the same wavelengths.

15. SUBJECT TERMS
Polycrystalline zinc selenide, semiconductor nonlinear optics, harmonic generation and mixing, ultrafast nonlinear optics

16. SECURITY CLASSIFICATION OF:			**17. LIMITATION OF ABSTRACT**	**18. NUMBER OF PAGES**	**19a. NAME OF RESPONSIBLE PERSON**
a. REPORT	**b. ABSTRACT**	**c. THIS PAGE**			Andrew Wharmby
U	U	U	SAR Unclassified	9	**19b. TELEPHONE NUMBER** *(include area code)* 210-539-8284

INSTRUCTIONS FOR COMPLETING SF 298

1. REPORT DATE. Full publication date, including day, month, if available. Must cite at least the year and be Year 2000 compliant, e.g. 30-06-1998; xx-06-1998-, xx-xx-1998.

2. REPORT TYPE. State the type of report, such as final, technical, interim, memorandum, master's thesis, progress, quarterly, research, special, group study, etc.

3. DATES COVERED. Indicate the time during which the work was performed and the report was written, e.g., Jun 1997 - Jun 1998; 1-10 Jun 1996; May - Nov 1998; Nov 1998.

4. TITLE. Enter title and subtitle with volume number and part number, if applicable. On classified documents, enter the title classification in parentheses.

Ba. CONTRACT NUMBER. Enter all contract numbers as they appear in the report, e.g. F33615-86-C-5169.

5b. GRANT NUMBER. Enter all grant numbers as they appear in the report, e.g. AFOSR-82-1234.

5c. PROGRAM ELEMENT NUMBER. Enter all program element numbers as they appear in the report, e.g. 61101A.

5d. PROJECT NUMBER. Enter all project nurnbers as they appear in the report, e.g. 1F665702D1257; ILIR.

5e. TASK NUMBER. Enter all task numbers as they appear in the report, e.g. 05; RF0330201; T4112.

5f. WORK UNIT NUMBER. Enter all work unit numbers as they appear in the report, e.g. 001; AFAPL30480105.

6. AUTHOR(S). Enter name(s) of person(s) responsible for writing the report, performing the research, or credited with the content of the report. The form of entry is the last name, first name, middle initial, and additional qualifiers separated by commas, e.g. Smith, Richard, J, Jr.

7. PERFORMING ORGANIZATION NAME(S) AND ADDRESS(ES). Self-explanatory.

8. PERFORMING ORGANIZATION REPORT NUMBER. Enter all unique alphanumeric report numbers assigned by the performing organization, e.g. BRL-1234; AFWL-TR-85-4017-Vol-21-PT-2.

9. SPONSORING/MONITORING AGENCY NAME(S) AND ADDRESS(ES). Enter the name and address of the organization(s) financially responsible for and monitoring the work.

10. SPONSOR/MONITOR'S ACRONYM(S). Enter, if available, e.g. BRL, ARDEC, NADC.

11. SPONSOR/MONITOR'S REPORT NUMBER(S). Enter report number as assigned by the sponsoring/ monitoring agency, if available, e.g. BRL-TR-829; -21 5.

12. DISTRIBUTION/AVAILABILITY STATEMENT. Use agency-mandated availability statements to indicate the public availability or distribution limitations of the report. If additional limitations/ restrictions or special markings are indicated, follow agency authorization procedures, e.g. RD/FRD, PROPIN, ITAR, etc. Include copyright information.

13. SUPPLEMENTARY NOTES. Enter information not included elsewhere such as: prepared in cooperation with; translation of; report supersedes; old edition number, etc.

14. ABSTRACT. A brief (approximately 200 words) factual summary of the most significant information.

15. SUBJECT TERMS. Key words or phrases identifying major concepts in the report.

16. SECURITY CLASSIFICATION. Enter security classification in accordance with security classification regulations, e.g. U, C, S, etc. If this form contains classified information, stamp classification level on the top and bottom of this page.

17. LIMITATION OF ABSTRACT. This block must be completed to assign a distribution limitation to the abstract. Enter UU (Unclassified Unlimited) or SAR (Same as Report). An entry in this block is necessary if the abstract is to be limited.

Research Article | Vol. 27, No. 3 | 4 Feb 2019 | OPTICS EXPRESS 2828
Optics EXPRESS

Eye safety implications of high harmonic generation in zinc selenide

CHRISTOPHER. B. MARBLE,[1,2,*] SEAN. P. O'CONNOR,[1,3] DAWSON. T. NODURFT,[1,3] ANDREW. W. WHARMBY,[4] AND VLADISLAV V. YAKOVLEV[1]

[1]*Texas A&M University, Department of Physics, 4242 TAMU, College Station, TX 77843, USA*
[2]*Consortium Research Fellows Program, 4214 King Street, First Floor Alexandria, Virginia 22302, USA*
[3]*Engility Corporation, 4241 Woodcock Dr. Ste. B-100, San Antonio, TX 78228, USA*
[4]*711th Human Performance Wing, Airman Systems Directorate, Bioeffects Division, Optical Radiation Branch, 4141 Petroleum Rd., JBSA Fort Sam Houston, TX 78234, USA*
**cmarble112@tamu.edu*

Abstract: Polycrystalline zinc selenide (ZnSe) has been the subject of many nonlinear optics studies for wavelengths under 4.0 µm including sum/difference frequency generation, harmonic generation, and filamentation. In this report, the conversion efficiency of high harmonic generation (HHG) in ZnSe is quantified for mid-infrared wavelengths ranging from 2.7 µm to 8.0 µm. By increasing the fundamental wavelength, we demonstrate that HHG in thick ZnSe targets is limited by the band gap. The high conversion efficiency of mid-infrared to near-infrared light in ZnSe raises concerns of a nonlinear retinal hazard. We contrast the HHG behavior of ZnSe against the observed harmonic generation of calcium fluoride, BK7, and fused silica over the same wavelengths.

1. Introduction

Polycrystalline zinc selenide (ZnSe) is utilized for applications ranging from harmonic generation [1] to broadband frequency conversion [2] due to its unusually strong nonlinear properties. Quasi-phase matching in polycrystalline ZnSe's crystal grains [3] has been used to explain enhanced sum [4] and difference frequency generation [3], second-harmonic generation [2,4,5], and extended phase matching conditions allowing for broadband frequency conversion [4,5]. Filamentation studies report that high intensity pulses generate visible blue filaments near the front surface of ZnSe windows [6,7] and that filamentation in ZnSe can result in the generation of a broadband supercontinuum, which can be seen in spectra between the strong harmonic peaks [5,8]. Despite the breath of studies of the nonlinear optical properties of ZnSe, we are not aware of a study to determine if the nonlinear frequency conversion of mid-infrared pulses in ZnSe could pose a retinal hazard.

In this report, the nonlinear behavior of three common optical materials (calcium fluoride (CaF_2), BK7 and UV-Vis grade fused silica) are contrasted against ZnSe. Prior studies of CaF_2 have reported a measurable third order susceptibility resulting in third harmonic generation, with fifth harmonic generation in CaF_2 believed to be a result of four wave mixing and not a fifth order susceptibility [9]. BK7 can generate second harmonic signals only from its surface due to its amorphous composition and has been observed to undergo third harmonic generation in the bulk media [10,11]. Like BK7, fused silica can undergo second harmonic generation at its surface [10] and third harmonic generation in the bulk media [12]. Higher odd harmonics up to 33rd order have been observed in fused silica when using a vacuum chamber [13].

HHG generation in semiconductors was, to our knowledge, first observed in zinc oxide (ZnO). Similar to ZnSe, ZnO was previously known to possess a strong nonlinearity attributed to its nanostructure [14]. In the HHG study of ZnO, harmonics, up to 25th order,

#347664 https://doi.org/10.1364/OE.27.002828
Journal © 2019 Received 22 Oct 2018; revised 29 Nov 2018; accepted 13 Dec 2018; published 29 Jan 2019

Optics EXPRESS

were generated using a 3.25 μm laser [15]. A later study observed even and odd HHG in gallium selenide using a 10.0 μm laser [16]. HHG in semiconductors has been approached theoretically using different methods [17] such as viewing single electron motion with a semiclassical model [15,18,19], solving the time-dependent Schrödinger equation [20,21], and taking the Hartree-Fock approximation while incorporating semiconductor Bloch equations [16,22]. HHG in ZnSe has been considered theoretically, concluding that HHG at 5.0 μm and 6.7 μm is dominated by emission from electron wave packets propagating along the Γ*L* and Γ*K* symmetry axes of the Brillouin zones with the Γ*L* symmetry axis providing stronger harmonic contributions for wavelengths below the bandgap [23]. N-th harmonic generation in ZnSe has been experimentally observed to obey an I_0^N power law dependence for intensities < 0.1 TW/cm^2 (the perturbative regime) and transitions to a clearly nonperturbative regime at higher intensities with the formation of a harmonic plateau [23].

The ease in which HHG can be generated with ZnSe raises questions about the possibility of a HHG driven retinal hazard. Studies of harmonic generation in ZnSe in the 1.5 μm – 2.4 μm range observed harmonics of second to fourth order [5], while studies using 3.0 μm, 3.9 μm, and 5.2 μm laser pulses resulted in observations of sixth, seventh and eighth harmonic generation respectively [1,24,25]. HHG up to twelfth harmonic at 5.0 μm and fifteenth harmonic at 6.7 μm have been successfully generated [23]. The harmonics reported in these studies span the visible and near-infrared, wavelengths that can propagate to the retina and cause retinal injury.

Eye safety standards, such as ANSI Z136.1-2014, have set maximum permissible exposure (MPE) limits for laser systems dependent on factors such as the laser's wavelength and pulse duration. The MPE limits for retinal exposure are much higher for mid-IR lasers compared to visible lasers of similar pulse duration because mid-IR radiation is strongly absorbed by the aqueous and vitreous humors of the eye before reaching the retina [26]. Safety standards such as ANSI do not account for nonlinear processes that change pulse wavelengths. HHG poses a risk of retinal injury for high intensity mid-IR laser systems since HHG can convert mid-IR radiation to visible as well as near-IR radiation whose retinal MPE is much lower (0.1 μJ/cm^2 for wavelengths between 400 nm and 1050 nm) [26]. In this letter, we observe and quantify the energy conversion of HHG in polycrystalline zinc selenide (ZnSe). We choose to study the eye safety risks of HHG in ZnSe over other materials because ZnSe based optics are commonly used in mid-IR experiments due to its transparency to mid-IR wavelengths and resistance to optical damage. We then contrast these HHG observations against the low energy conversion observed in CaF_2, BK7 and UV-Vis grade fused silica under similar conditions. Since our initial presentation at the SPIE Photonics West conference [27], two studies have been conducted that suggest the conversion efficiency of ZnSe is unusually strong. The first study, reported after this letter's submission, showed frequency conversion in ZnSe to be efficient enough that the fundamental pulse can be depleted until the second harmonic intensity exceeds the fundamental pulse intensity [28]. The second study has presented preliminary results at the Frontiers of Optics conference reporting conversion efficiencies of 18-20% for a 5 mm ZnSe target and 26-28% for a 4 mm ZnSe target for mid-infrared wavelengths ranging from 3.3 μm to 3.8 μm [29] far in excess of the < 1% conversion efficiencies reported in other materials [30,31]. To our knowledge, this letter details the first systematic study of the HHG conversion efficiency of ZnSe for mid-IR wavelengths.

2. Methods

Tunable mid-IR, 1 kHz laser pulses were created using difference frequency generation of the signal and idler waves of an optical parametric amplifier (OPA). The OPA was pumped by an 800 nm, 80 fs Ti:sapphire laser (SpitFire by Spectra-Physics). The resulting mid-IR pulses have a nominal pulse duration of 80 fs. The OPA (Light Conversion TOPAS Twins model TT8F12C1) could be tuned to produce excitation wavelengths from 2.7 μm to 12 μm with a

Optics EXPRESS

maximum pulse energy of 18 µJ ± 2 µJ at 3.5 µm. The mid-IR beam diameter was 3.0 mm. Leakage of the signal, idler and pump frequencies was observed in the beam spectra, so the beam was passed through two dichroic mirrors to minimize these undesired contributions. The knife edge technique was used to find the beam diameters and the pulse energies were measured using a Coherent EM USB J-10MB-LE power meter.

HHG in ZnSe was achieved by focusing the mid-IR laser pulse into a 10-mm thick polycrystalline ZnSe window using a 40-mm CaF_2 lens (see Fig. 1). For each wavelength, the harmonics generated were recorded using two Ocean Optics spectrometers (the USB 2000 + model for visible wavelengths and the NIR-512 model for near-IR wavelengths). HHG spectra were taken for excitation wavelengths between 2.7 µm to 3.0 µm at 0.1-µm increments, and from 3.0 µm to 8.0 µm at 0.5-µm increments. For each wavelength, the ZnSe window was moved into the focal point and the 75 mm collection optic adjusted to maximize the signal recorded by the visible spectrometer. The position of the ZnSe window was adjusted to optimize the signal from the highest harmonic peak observed. After measuring the signals, visible and near-IR spectra without the ZnSe window in the beam path were taken to verify that leakage of the signal, idler or pump frequencies from the OPA were not contributing to the observed spectra.

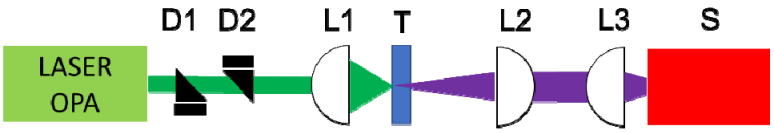

Fig. 1. The first experimental setup. D1 and D2 are dichroic mirrors, L1-L3 are Eksma Optics™ lenses (models 110-5204E, 110-5209E, and 110-5205E respectively). T is the ZnSe target and S is the USB 2000 + or NIR-512 spectrometer. The Ti:sapphire pump and regenerative amplifier (Spectra Physics Spitfire Ace model 8PTFPA-100F-1K-ACE) are not shown.

The UV-grade fused silica window cracked when exposed to 2.8 µm – 3.0 µm pulses, most likely a result of a rapid rise in temperature due to strong absorption resulting in thermal expansion which cracked the glass. A filter wheel was added to reduce the peak intensity to avoid damaging the fused silica window (see Fig. 2). The laser was committed to other experiments at the time so measurements of the CaF_2, BK7, and UV-grade fused silica windows (models CF-W-50-3, PW-1037-C and PW-1037-UV with thicknesses of 3.0 mm, 10.0 mm and 10.0 mm respectively) were taken with a beam expander in the beam path (see Fig. 2). Harmonic generation in the three windows was measured with the Ocean Optics USB 2000 + and NIR-512 spectrometers using the same procedure discussed above for ZnSe. New reference measurements without the windows were taken for the modified setup.

The absolute efficiencies of the USB 2000 + and NIR-512 were estimated using an Ocean Optics LS-1 light source. The relative efficiencies were calculated by measuring the spectral distribution of the LS-1 light source propagated through the collection optics, and approximating the actual spectral distribution of the LS-1 as a black body at a temperature of 3100 K. The relative efficiencies were then converted to absolute efficiencies using the LS-1 light source's power as reported by a Coherent PowerMax PM10. By summing over the absolute efficiency curve, the percentage of the initial pulse energy converted to wavelengths under 1200 nm (which are a direct retinal hazard) could be estimated.

Optics EXPRESS

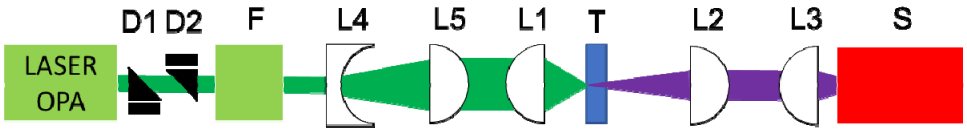

Fig. 2. The second experimental setup. F is the filter wheel. L1-L5 are Eksma Optics™ lenses (models 110-5204E, 110-5209E, 110-5205E, 112-5217E, and 561-6265 respectively). T is the target media (CaF_2, BK7 or fused silica). D1, D2, and S remain unchanged from Fig. 1.

3. Results and discussion

At the maximum beam intensity at 3.0 µm, HHG in ZnSe generated a red beam visible to the unaided eye. A reflected blue spot was observed when the front surface of the ZnSe window was moved through the focal point for excitation wavelengths of 2.9 µm – 3.5 µm, consistent with filamentation reported in [6]. However, blue light was not visible in the exiting beam or measured by the visible spectrometer. This is most likely explained by the strong absorption of harmonic wavelengths in ZnSe below 500 nm due to the band gap at 2.71 eV. The collected signal was found to be maximized when the beam was focused into the front surface of the ZnSe window. Nevertheless, HHG could still be detected when focusing into the bulk media.

The intensity of the visible harmonics oversaturated the USB 2000 + spectrometer in the 2.7 µm to 5.5 µm excitation range, so ND filters were placed between the L3 optic (see Fig. 1) and the spectrometer. The ZnSe spectra for excitation wavelengths of 5.0 µm and 7.0 µm are plotted in Figs. 3(a) and 3(b) respectively. The intensities are reported after subtracting background measurements of visible light leakage from the OPA. The intensities recorded by the USB 2000 + in Fig. 3 were initially a factor of six lower than the intensities recorded by the NIR-512 in the overlapping wavelength range, consistent with the difference in detector wavelength bin sizes. Optimization of the alignment of the ZnSe window and collection optic for the 5.5 µm to 8.0 µm excitation measurements using the USB 2000 + were unsuccessful due to the long integration times between adjustments, resulting in a lower count rate. The count rates for the USB 2000 + in Fig. 3 have been raised to correct for the use of ND filters, bin size difference and, in the case of Fig. 3(b) where optimization was not possible, to be consistent with the NIR-512 measurement in the overlapping region.

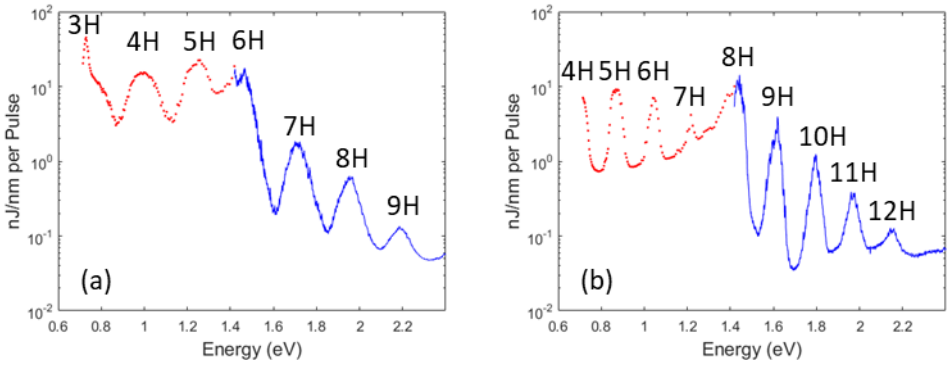

Fig. 3. Zinc selenide spectra for a (a) 5.0 µm beam and (b) 7.0 µm beam. Red data (dots) shows the near-IR spectra measured with the NIR-512. Blue data (line) shows the visible spectra measured with the USB 2000 + .

Consistent with literature, we observed harmonic generation for 3.0 µm to 5.0 µm excitation wavelengths for ZnSe with the harmonics terminating near the band gap energy.

Optics EXPRESS

The exiting pulses contained a substantial fraction of light in the near-infrared below 1200 nm with values ranging from (8 ± 6) % to (21 ± 14) % of the initial pulse energy (see Table 1).

This corresponds to visible and near-infrared exposures of (1.2 ± 0.8) μJ to (2.3 ± 1.6) μJ of energy, more than sufficient to pose a retinal hazard under the ANSI standard. From Figs. 3(b) and 4 we were able to achieve visible wavelength HHG at excitation wavelengths longer than 5.0 μm consistent with the HHG reported in [23]. For excitation wavelengths above 8.0 μm, the HHG spectra could no longer be observed. This is consistent with expectations because the peak intensity decreases rapidly beyond 8.0 μm due to increasing absorption of the calcium fluoride optics and the increasing beam radius at longer wavelengths (see Table 1). Estimating the visible pulse energy from the USB 2000 + measurements for excitation wavelengths longer than 5.0 μm requires adjusting the spectra to correct for misalignment, as discussed above for Fig. 3(b). Even increasing the fundamental wavelength to 7.5 μm, we were able to convert (13 ± 9) % of the pulse energy into sub-1200 nm radiation more than sufficient to pose an eye hazard under the ANSI standard (assuming a recollimated 3.0 mm beam diameter). Harmonics wavelengths below 460 nm were absent for all measured wavelengths and only weak unconfirmed peaks were observed for wavelengths between 460 nm to 500 nm, which was consistent with the increased absorption of harmonic wavelengths shorter than 500 nm in ZnSe and the thickness of the sample.

Table 1. Beam Properties for Zinc Selenide Study.

Wavelength (μm)	Pulse Energy (μJ)	Beam Radius (μm)	Intensity (GW/cm^2)	Energy Converted to sub-1.2 μm Wavelengths (%)*
2.7	7.1 ± 0.7	45 ± 5	1400 ± 400	15 ± 11
2.8	11 ± 1	47 ± 5	2000 ± 500	15 ± 11
2.9	15 ± 2	49 ± 6	2500 ± 600	15 ± 11
3.0	17 ± 2	50 ± 6	2700 ± 700	11 ± 7
3.5	18 ± 2	59 ± 7	2100 ± 500	11 ± 8
4.0	14 ± 1	67 ± 8	1200 ± 300	8 ± 6
4.5	13 ± 1	76 ± 9	900 ± 200	10 ± 7
5.0	11 ± 1	80 ± 10	600 ± 200	21 ± 14
5.5	8.7 ± 0.9	90 ± 10	400 ± 100	28 ± 20
6.0	6.4 ± 0.6	100 ± 10	250 ± 60	29 ± 20
6.5	5.4 ± 0.5	110 ± 10	180 ± 50	27 ± 19
7.0	4.9 ± 0.5	120 ± 10	140 ± 40	13 ± 9
7.5	4.4 ± 0.4	130 ± 10	110 ± 30	13 ± 9
8.0	3.2 ± 0.3	130 ± 20	70 ± 20	2.8 ± 2.0

* The large uncertainties reported are derived from the calibration measurement including the approximation of the LS-1 spectra as a blackbody, poor agreement between the visible and infrared spectrometers in the overlapping region and the poor collimation of the LS-1 light source

Optics EXPRESS

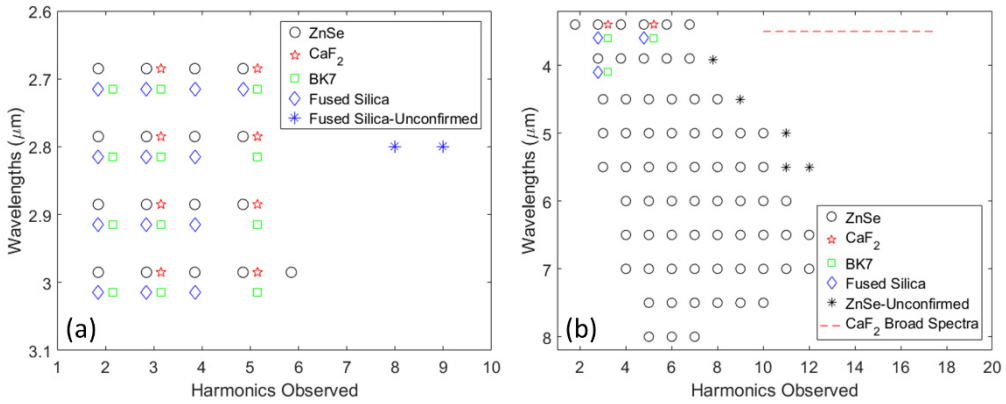

Fig. 4. (a) the harmonics observed for wavelengths from 2.7 μm to 3.0 μm. (b) the harmonics observed for wavelengths from 3.5 μm to 8.0 μm.

These results contrast with observations for CaF_2, BK7, and fused silica. All three materials required longer integration times than ZnSe and none oversaturated the visible detector. The fraction of pulse energy converted to sub-1.2 nm wavelengths was commonly on the order of 10 nJ (< 1% the input pulse energy), with the highest efficiency conversion of (2.2 ± 1.5) % observed using a 2.9 μm beam for fused silica. The CaF_2 was observed to generate third and fifth harmonics consistent with literature (Figs. 4 and 5). Unlike ZnSe, CaF_2 did not generate measurable harmonics for excitation wavelengths greater than 3.5 μm despite ZnSe generating third harmonic up to the detector cutoff using a 5.5 μm beam and fifth harmonic using an 8.0 μm beam (Fig. 4(b)). Placing the front surface of the BK7 window in the focal point resulted in measurable second harmonic, as well as third and fifth harmonic, but at much lower count rates than ZnSe. Higher harmonics were not observed at any wavelength in BK7. Fused silica generated measurable second, third, and fourth harmonics (for excitation wavelengths from 2.7 μm to 3.0 μm). Since a UV-grade fused silica window was used, the front surface of the window had to be placed at the focus to avoid absorption prior to harmonic generation. We observed fifth harmonic generation using a 2.7 μm and a 3.5 μm beam, but were not able to measure the fifth harmonic at 2.8 μm to 3.0 μm. Likewise, we observed weak signals at higher harmonics using a 2.8 μm beam, but did not observe these signals at any other wavelength tested (see Fig. 4). We observe that fourth harmonic generation only occurred in UV-grade fused silica at excitation wavelengths whose bandwidth covered the -OH resonance. We attribute the fourth harmonic generation at those wavelengths to -OH overtone enhanced bulk quadrupole effect. At 3.5 μm, past the -OH resonance, fused silica generates third and fifth harmonics similar to BK7.

Optics EXPRESS

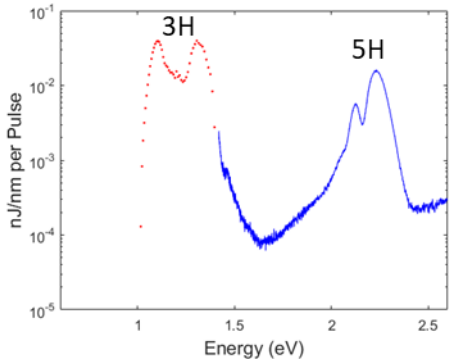

Fig. 5. CaF_2 spectra for a 3.0 µm beam. Red data (dots) shows the near-IR spectra measured with the NIR-512. Blue data (line) shows the visible spectra measured with the USB 2000 + . Both sets are plotted after subtracting the background without the CaF_2 target.

Table 2. Beam Parameters for CaF_2, Fused Silica, and BK7.

Wavelength (µm)	Pulse Energy (µJ)	Beam Radius (µm)	Intensity (GW/cm^2)
2.7	2.7 ± 0.3	40 ± 4	700 ± 200
2.8	4.9 ± 0.5	40 ± 4	1200 ± 400
2.9[a]	3.5 ± 0.4	47 ± 5	600 ± 200
2.9[b]	7.0 ± 0.7	47 ± 5	1300 ± 300
3.0[a]	4.3 ± 0.4	43 ± 4	900 ± 300
3.0[b]	8.0 ± 0.8	43 ± 4	1700 ± 500
3.5	6.6 ± 0.7	68 ± 7	600 ± 100
4.0	4.0 ± 0.4	77 ± 8	270 ± 60
4.5	3.6 ± 0.4	71 ± 7	280 ± 80

[a]For CaF_2 and Fused Silica measurements (energy reduced to prevent damage to fused silica). [b]For BK7 measurements (energy not reduced).

4. Conclusion

We performed a systematic study of HHG in ZnSe using excitation pulses from 2.7 µm to 8.0 µm resulting in HHG at wavelengths not previously studied and the generation of HHG up to twelfth order. We demonstrate that the band gap wavelength acts as an upper limit of efficient harmonic generation in polycrystalline ZnSe. The production of high harmonics in ZnSe corresponds with substantial frequency conversion, with conversions of (8 ± 6) % to (29 ± 20) % in the sub-1.2 µm range. The generation of (2.3 ± 1.6) µJ of sub-1.2 µm radiation using a sub-20 µJ mid-infrared laser suggests that the use of ZnSe optics may pose an unexpected retinal hazard for high intensity mid-infrared laser applications. If the beam had been recollimated to a 3.0 mm diameter, the sub-1.2 µm energy per unit area of the beam would approach (30 ± 20) µJ/cm^2, well above the ANSI MPE limits (0.1 µJ/cm^2 for sub-1050 nm pulses to 0.8 µJ/cm^2 for 1200 nm pulses) [26]. The efficient conversion of mid-infrared to near-infrared radiation in ZnSe is contrasted by the behavior of other materials whose conversion efficiencies are typically below 1% and is supported by parallel studies reported this year [28,29]. By contrasting ZnSe against fused silica, calcium fluoride, and BK7 this study further emphasizes that harmonic generation in semiconductors is the result of a different process than in other solid optical materials.

Funding

Consortium Research Fellows Program (CRFP); Engility Corporation; Air Force Research Laboratory (AFRL); Herman F. Heep and Minnie Belle Heep Texas A&M University Endowed Fund; National Science Foundation (DBI-1455671, DBI-1532188, ECCS-1509268,

Optics EXPRESS

CMMI-1826078); National Science Foundation Graduate Research Fellowship Program (Award No. DGE 1746932), Air Force Office of Scientific Research (AFOSR) (FA9550-18-1-0141, FA9550-15-1-0517); DARPA funding through a sub-contract from AFRL (FA8650-13-D-6368/0006); National Institutes of Health (NIH) (1R01GM127696-01); Office of Naval Research (ONR) (N00014-16-1-2578); Robert A. Welch Foundation (A-1261)

Acknowledgments

The authors thank Mr. Gary Noojin and Mr. Joseph Clary for their assistance in setting up this experiment. Sean O'Connor thanks Dr. Marlan O. Scully for his funding and support.

This material is based upon work supported by the National Science Foundation Graduate Research Fellowship Program under Grant No. DGE 1746932. Any opinions, findings, and conclusions or recommendations expressed in this material are those of the authors and do not necessarily reflect the views of the National Science Foundation.

Distribution A: Approved for public release; distribution unlimited. PA Case No: TSRL-PA-2018-0212. The opinions expressed on this document, electronic or otherwise, are solely those of the author(s). They do not represent an endorsement by or the views of the United States Air Force, the Department of Defense, or the United States Government.

References

1. A. H. Chin, O. G. Calderón, and J. Kono, "Extreme midinfrared nonlinear optics in semiconductors," Phys. Rev. Lett. **86**(15), 3292–3295 (2001).
2. A. Saha and S. Deb, "Broadband second-harmonic generation in the near-infrared region in a tapered zinc selenide slab using total internal reflection quasi-phase matching," Jpn. J. Appl. Phys. **50**(10R), 102201 (2011).
3. M. Baudrier-Raybaut, R. Haïdar, P. Kupecek, P. Lemasson, and E. Rosencher, "Random quasi-phase-matching in bulk polycrystalline isotropic nonlinear materials," Nature **432**(7015), 374–376 (2004).
4. T. D. Chinh, W. Seibt, and K. Siegbahn, "Dot patterns from second-harmonic and sum-frequency generation in polycrystalline ZnSe," J. Appl. Phys. **90**(5), 2612–2614 (2001).
5. R. Šuminas, G. Tamošauskas, G. Valiulis, V. Jukna, A. Couairon, and A. Dubietis, "Multi-octave spanning nonlinear interactions induced by femtosecond filamentation in polycrystalline ZnSe," Appl. Phys. Lett. **110**(24), 241106 (2017).
6. A. Dubietis, G. Tamošauskas, R. Šuminas, V. Jukna, and A. Couairon, "Ultrafast supercontinuum generation in bulk condensed media," Lith. J. Phys. **57**(3), 113–157 (2017).
7. M. Durand, A. Houard, K. Lim, A. Durécu, O. Vasseur, and M. Richardson, "Study of filamentation threshold in zinc selenide," Opt. Express **22**(5), 5852–5858 (2014).
8. O. Mouawad, P. Béjot, F. Billard, P. Mathey, B. Kibler, F. Désévédavy, G. Gadret, J.-C. Jules, O. Faucher, and F. Smektala, "Filament-induced visible-to-mid-IR supercontinuum in a ZnSe crystal: Towards multi-octave supercontinuum absorption spectroscopy," Opt. Mater. **60**, 355–358 (2016).
9. N. Garejev, I. Gražulevičiūtė, D. Majus, G. Tamošauskas, V. Jukna, A. Couairon, and A. Dubietis, "Third- and fifth-harmonic generation in transparent solids with few-optical-cycle midinfrared pulses," Phys. Rev. A **89**(3), 033846 (2014).
10. F. J. Rodriguez, F. X. Wang, and M. Kauranen, "Calibration of the second-order nonlinear optical susceptibility of surface and bulk of glass," Opt. Express **16**(12), 8704–8710 (2008).
11. W. Liu, L. Wang, F. Han, and C. Fang, "Distinct broadband third-harmonic generation on a thin amorphous medium-air interface," Opt. Lett. **38**(17), 3304–3307 (2013).
12. U. Gubler and C. Bosshard, "Optical third-harmonic generation of fused silica in gas atmosphere: Absolute value of the third-order nonlinear optical susceptibility $\chi(3)$," Phys. Rev. B Condens. Matter Mater. Phys. **61**(16), 10702–10710 (2000).
13. Y. S. You, Y. Yin, Y. Wu, A. Chew, X. Ren, F. Zhuang, S. Gholam-Mirzaei, M. Chini, Z. Chang, and S. Ghimire, "High-harmonic generation in amorphous solids," Nat. Commun. **8**(1), 724 (2017).
14. G. I. Petrov, V. I. Shcheslavskiy, I. Ozerov, E. Chelnokov, V. I. Marine, and V. V. Yakovlev, "Extremely efficient direct third harmonic generation in thin nanostructured films of ZnO," Proc. SPIE **5337**, 166–172 (2004).
15. S. Ghimire, A. D. DiChiara, E. Sistrunk, G. Ndabashimiye, U. B. Szafruga, A. Mohammad, P. Agostini, L. F. DiMauro, and D. A. Reis, "Generation and propagation of high-order harmonics in crystals," Phys. Rev. A **85**(4), 043836 (2012).
16. O. Schubert, M. Hohenleutner, F. Langer, B. Urbanek, C. Lange, U. Huttner, D. Golde, T. Meier, M. Kira, S. W. Koch, and R. Huber, "Sub-cycle control of terahertz high-harmonic generation by dynamical Bloch oscillations," Nat. Photonics **8**(2), 119–123 (2014).

Optics EXPRESS

17. T. T. Luu and H. J. Wörner, "High-order harmonic generation in solids: A unifying approach," Phys. Rev. B **94**(11), 115164 (2016).
18. M. W. Feise and D. S. Citrin, "Semiclassical theory of terahertz multiple-harmonic generation in semiconductor superlattices," Appl. Phys. Lett. **75**(22), 3536–3538 (1999).
19. O. D. Mücke, "Isolated high-order harmonics pulse from two-color-driven Bloch oscillations in bulk semiconductors," Phys. Rev. B Condens. Matter Mater. Phys. **84**(8), 081202 (2011).
20. M. Wu, S. Ghimire, D. A. Reis, K. J. Schafer, and M. B. Gaarde, "High-harmonic generation from Bloch electrons in solids," Phys. Rev. A **91**(4), 043839 (2015).
21. P. G. Hawkins, M. Y. Ivanov, and V. S. Yakovlev, "Effect of multiple conduction bands on high-harmonic emission from dielectrics," Phys. Rev. A **91**(1), 013405 (2015).
22. D. Golde, T. Meier, and S. W. Koch, "High harmonics generated in semiconductor nanostructures by the coupled dynamics of optical inter- and intraband excitations," Phys. Rev. B Condens. Matter Mater. Phys. **77**(7), 075330 (2008).
23. A. A. Lanin, E. A. Stepanov, A. B. Fedotov, and A. M. Zheltikov, "Mapping the electron band structure by intraband high-harmonic generation in solids," Optica **4**(5), 516–519 (2017).
24. G. M. Archipovaite, S. Petit, J. C. Delagnes, and E. Cormier, "100 kHz Yb-fiber laser pumped 3 μm optical parametric amplifier for probing solid-state systems in the strong field regime," Opt. Lett. **42**(5), 891–894 (2017).
25. T. Kanai, P. Malevich, S. S. Kangaparambil, K. Ishida, M. Mizui, K. Yamanouchi, H. Hoogland, R. Holzwarth, A. Pugzlys, and A. Baltuska, "Parametric amplification of 100 fs mid-infrared pulses in $ZnGeP_2$ driven by a Ho:YAG chirped-pulse amplifier," Opt. Lett. **42**(4), 683–686 (2017).
26. *American National Standard for Safe Use of Lasers: ANSI Z136.1–2014* (Laser Institute of America, 2014).
27. C. B. Marble, S. P. O'Connor, D. T. Nodurft, V. V. Yakovlev, and A. W. Wharmby, "Zinc selenide: an extraordinarily nonlinear material," Proc. SPIE **10528**, 105281X (2018).
28. R. Šuminas, A. Marcinkevičiūtė, G. Tamošauskas, and A. Dubietis, "Even and odd harmonics-enhanced supercontinuum generation in zinc-blende semiconductors," J. Opt. Soc. Am. B **36**, A22–A27 (2019).
29. K. Werner, N. Talisa, B. Wilmer, L. Vanderhoef, A. Schweinsberg, C. Wolfe, A. Valenzuela, and E. Chowdhury, "Mid-Wave Infrared Nonlinear Optics in Polycrystalline Zinc Selenide and Zinc Sulfide," in Frontiers in Optics 2018, OSA Technical Digest (Optical Society of America, 2018), paper JTu3A.33.
30. S. Gholam-Mirzaei, J. Beetar, and M. Chini, "High harmonic generation in ZnO with a high-power mid-IR OPA," Appl. Phys. Lett. **110**(6), 061101 (2017).
31. D. D. Hickstein, D. R. Carlson, A. Kowligy, M. Kirchner, S. R. Domingue, N. Nader, H. Timmers, A. Lind, G. G. Ycas, M. M. Murnane, H. C. Kapteyn, S. B. Papp, and S. A. Diddams, "High harmonic generation in periodically poled waveguides," Optica **4**(12), 1538–1544 (2017).